Determination of Exciton Diffusion Coefficient in Conjugated Polymer Films: Novel Method based on Spectroelectrochemical Techniques

Francisco Montilla[1], *Andrés F. Quintero-Jaime*[1], *Francisco Huerta*[2], *César Quijada*[2]

[1] Departamento de Química Física e Instituto Universitario de Materiales de Alicante. Universidad de Alicante. Apdo. de Correos 99, E-03080 Alicante, Spain

[2] Departamento de Ingenieria Textil y Papelera, Universitat Politècnica de València, Plaza Ferrandiz y Carbonell, 1, E-03801 Alcoy, Spain.

francisco.montilla@ua.es

Abstract

The understanding of exciton dynamics is a central issue in the operation of conjugated polymer-based optoelectronic devices, like solar cells, light-emitting diodes or electrochemiluminescent cells. In this work, we explore the applicability of combined *in situ* electrochemical fluorescence and UV-vis spectroscopies for the study of electrochemically induced quenching of photoluminescence as novel tools for the determination of exciton diffusion in a model conjugated polymer, poly[2-methoxy-5-(2-ethylhexyloxy)-1,4-phenylvynilene] (MEH-PPV). It is demonstrated that the quenching process observed upon electrochemical doping follows a linear Stern-Volmer mechanism at low doping levels, with a time-independent rate constant typical of diffusion-controlled annihilation processes. From the Stern-Volmer rate constant and the exciton-polaron critical distance, an exciton diffusion coefficient is derived whose value is in close agreement with those reported in the literature. These results support the suitability of these spectroelectrochemical techniques as fast and powerful alternative tools for the reliable determination of exciton diffusion coefficients in conjugated polymers.

1. Introduction

Exciton dynamics play a central role in the operation of most organic optoelectronic devices. These processes are critical in working OLEDs, organic photovoltaic cells or luminescent electrochemical cells [1,2]. For example, in organic photovoltaic cells, the photogenerated excitons must move to interfacial zones to be dissociated into charge carriers and, consequently, large exciton diffusion lengths are required to enhance efficiency. A major part of these devices is based on conjugated polymers since they are attractive for the high amount of processing techniques that allow their use as thin films in flexible and lightweight substrates.

The process of exciton diffusion in polymer films can be characterized either by spectroscopic techniques, which measure the efficiency of radiated photons in the presence of quenchers or by charge carrier techniques, which measure photogenerated charges resulting from quenched excitons [3]. Among the spectroscopic techniques, those based on the quenching of photoluminescence are widely extended. The photoluminescence (PL) of thin films is measured in the absence and in the presence of a quenching site and the exciton diffusion length is derived from the PL quotient. In these studies, a statistically significant number of experiments are required to obtain consistent results and therefore many samples must be prepared. Typical quenchers include electron acceptors as fullerene-C_{60}, subphtalocyanines or molecular dyes, prepared as interfacial films or blended with the polymer in bulk heterojunction architectures [4–6].

The electronic structure of conjugated polymers can be modified through a reversible electrochemical charge injection, which leads to the formation of charged states, such as polarons, polaronic bands or bipolarons, among others [7]. By coupling an electrochemical excitation system to a suitable spectroscopic technique, the spectral features of those excited

states can be characterized. In particular, electrochemical *in situ* UV-vis spectroscopy has been used to obtain the energy of the intragap transition in doped conjugated polymers and to quantify polaron absorption cross-sections, which are key parameters used for the development of electrically pumped lasers and for the optimization of organic light-emitting diodes, among other applications [8,9]

A related spectroelectrochemical technique, the electrochemical *in situ* fluorescence spectroscopy (also known as electrofluorochromism [10]) is a relatively novel tool that has been applied to the characterization of luminescent molecular systems and to the development of novel optoelectronic devices [11–15]. The use of electrochemical instrumentation allows fine and precise control of the quencher concentration permitting simultaneous analysis of exciton dynamics within a single sample of the conjugated polymer [16–18].

In the present work, a combination of electrochemical *in situ* steady-state fluorescence spectroscopy and UV-vis spectroscopy has been employed for the first time to determine the diffusion coefficient of excitons. The material selected for this study is the orange-red emitter MEH-PPV. Among the family of conjugated PPV polymers, it constitutes an archetypical material showing a huge variety of optoelectronic applications [19,20].

2. Experimental section

2.1. Materials

MEH-PPV was purchased from Sigma-Aldrich (average Mn 150000-250000). Fluorine-doped tin oxide (FTO)-coated glass substrates (FTO-AGC 80, 70−90 Ω) employed as electrode support in all the *in situ* spectroelectrochemical experiments was provided by SOLEMS. Anhydrous tetrahydrofuran (THF, ≥99.9%), anhydrous acetonitrile (ACN,

≥99.8%), tetrabutylammonium tetrafluoroborate (TBATFB ≥99%) and ferrocinium hexafluorophosphate (Fc, ≥97%) were supplied by Sigma-Aldrich.

2.2. In situ spectroelectrochemical characterization

In situ spectroelectrochemical measurements (absorption, steady-state PL), were performed in a modified, 1 cm length, fused silica cell capped with a Teflon plate, which also served as the electrode support [21]. Working electrode was prepared with FTO modified with a polymer film of MEH-PPV. Prior to the polymer deposition, FTO electrodes were cleaned by sonication in an acetone bath. Afterwards, 20 μL of MEH-PPV previously dissolved in THF (2.0 mg mL^{-1}) were drop-casted over $1cm^2$ of the FTO substrate. This working electrode was immersed in a solution of 0.1 M TBATFB in ACN. The counter electrode was a platinum wire and a silver wire was used as the pseudoreference electrode, both immersed in the same solution and protected by a glass capillary tube. The reference electrode was calibrated using the ferricenium/ferrocene redox couple (Fc/Fc^+). Air was purged from the electrochemical cell by bubbling with an argon flow for 10 min and the inert atmosphere was maintained during all the experiments.

Electrochemical experiments were carried out by using a function generator (EG&G Parc model 175) connected to a potentiostat-galvanostat (Pine Instrument model AFCBP1). Photoluminescence (PL) and UV-vis spectra were acquired using a PTI QuantaMaster spectrofluorometer (model QM-62003SE) and an Ocean Optics spectrophotometer (Flame model Avantes DH-2000-S and optical fibers Ocean Optics QP100-2-UV/VIS GF052107-101), respectively. The density of the polymer was determined by helium

microultrapicnometry (QUANTACHROME INSTRUMENTS) obtaining a value of 1.176 g cm^{-3} for the solid polymer. Resulting electrochemically-induced absorption (ECIA) UV-vis spectra for MEH-PPV films were obtained as follows. A first single reference spectrum was acquired at the E_{onset}, representing the electronic state of the neutral (undoped) film. Then, sample spectra were collected at increasing applied potentials, E_{app}, representing the electronic state of the polymer at different oxidation states during the *p*-doping process. Finally, the unique reference spectrum was subtracted from each sample spectra and the resulting absorbance change, ΔA, is plotted against wavelength. *In situ* fluorescence measurements were performed in a modified fluorescence cell (1 cm length quartz cell). Details on the cell design have been shown in a previous article [21].

3. Results and discussion

3.1. Optical and electrochemical characterization

Fig. 1.a shows the absorption (black curve) and the PL emission (red curve) spectra of a MEH-PPV polymer deposited as a thin film onto an FTO electrode. The absorption maximum at 505 nm corresponds to the $\pi\pi^*$ transition of conjugated chains, whereas the fluorescent emission displays a maximum at 594 nm and a well-defined vibronic feature at around 637 nm.

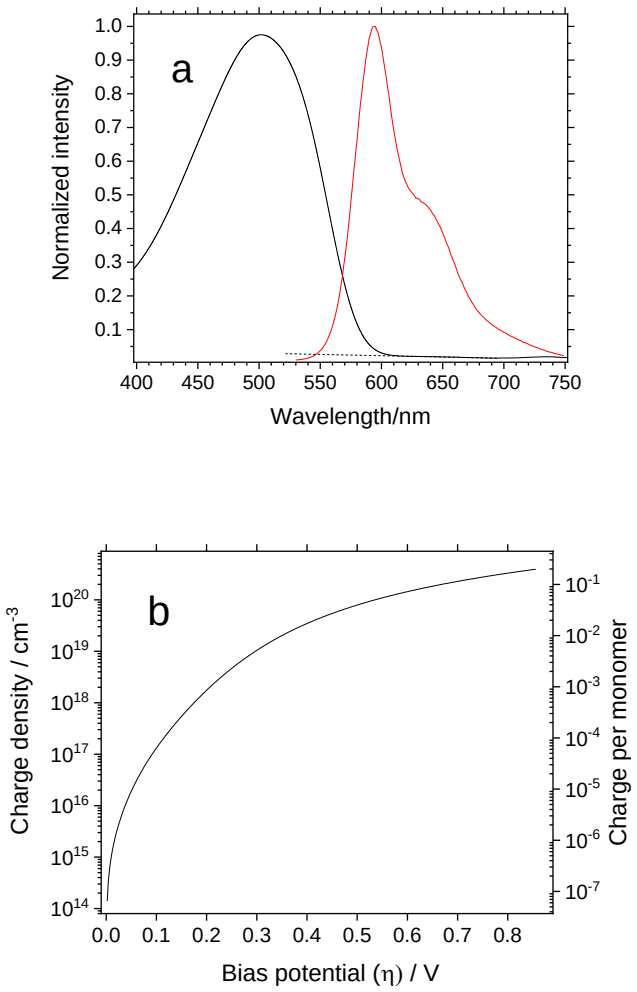

Figure 1: Absorption and emission spectra (λ_{exc}= 500 nm) of MEH-PPV films on FTO electrodes. b) Injected charge as a function of the bias potential applied over the onset of the *p*-doping process.

Since MEH-PPV is an electroactive material, it undergoes reversible doping by electrochemical methods. Fig. S1 in the supporting information shows the cyclic voltammogram of MEH-PPV including the reversible *p*- and *n*-doping processes in the polymer. Formation of positive polaronic species (*p*-doping) along the polymer chains starts

at around E_{onset}= -0.6 V, derived from the onset potential of the oxidation current recorded during the forward sweep. In the reverse scan, a reduction feature peaking at around -0.7 V appears in the CV, which corresponds to the dedoping of oxidized MEH-PPV. The electrochemical processes associated to *n*-doping of the polymer are observed in the left branch of the voltammetric curve. In the scan to negative potentials, *n*-doping starts at a reduction onset potential of –2.6 V, while reversible dedoping occurs with an oxidation peaking at around -2.6 V, after scan reversal. Since the oxidation onset for *p*-doping and the reduction onset of the *n*-doping corresponds to the energy of HOMO and LUMO levels of conjugated chains, respectively, the so-called electrochemical bandgap can be obtained easily from CV curves [22,23]. In the present case, the HOMO-LUMO difference calculated from the experiment in Fig. S1 amounts to 1.97 eV, in close agreement with those 2.00 eV measured for the optical bandgap obtained from the onset of the red-edge ππ* absorption band.

Fig 1.b shows the concentration of charges electrochemically injected within the film (i.e. the charge density) and the resulting number of charges per monomer unit against the bias potential. The presented bias potential, η, refers to the difference between the applied potential at each point and the onset potential for *p*-doping, $\eta=(E_{app} - E_{onset})$.

3.2. Spectroelectrochemical characterization of exciton diffusion

Electrochemically-induced absorption (ECIA) UV-vis spectroscopy is an experimental tool that provides valuable information on optoelectronic alterations triggered by the applied potential. The resulting ECIA-UV-vis spectra for MEH-PPV films are shown in Fig. 2.a.

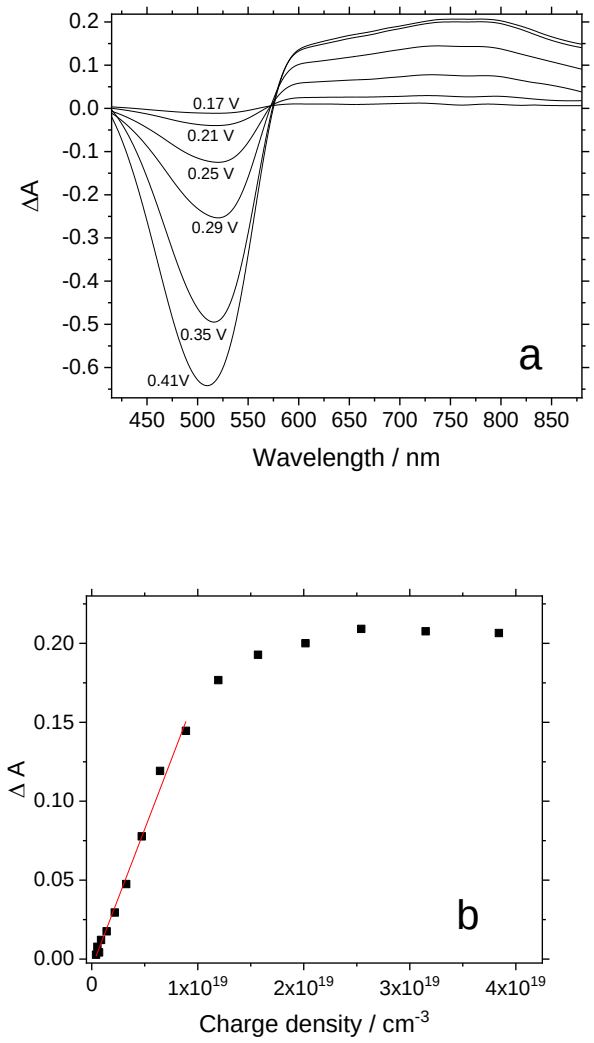

Figure 2. a) Electrochemically induced UV-vis spectra obtained during the *p*-doping process of MEH-PPV (bias potential is indicated close to each curve). b) Absorbance change of the electrochemically-induced UV-vis polaron transition band at increasing levels of *p*-doping.

As the bias potential increases, a negative absorption band appears at 517 nm corresponding to the bleaching of $\pi\pi^*$ transition. Concurrently, a wide positive absorption band develops at around 760 nm at increasing doping levels. The energy of the feature is compatible with an electron hop between the HOMO level and higher subgap states of polarons in MEH-PPV [24,25]. Fig. 2.b shows the change in the polaron peak intensity against the injected charge. At low doping levels the intensity of the transition increases almost linearly up to 1×10^{19} cm^{-3} (η=0.30 V), thus providing a method to determine the polaron absorption cross-section, σ, by means of Eq. 1 [8].

$$\sigma = \frac{2.30}{l}\frac{\Delta A}{\Delta CD} \qquad (1)$$

where ΔA is the electrochemically induced absorbance change, CD is the concentration of charge injected within the film and l is the film thickness. An absorption cross-section of 1.18×10^{-15} cm^2 is obtained, in agreement with literature data [26,27]. The saturation of the polaron band occurs from a charge density close to 2×10^{19} cm^{-3}, which corresponds to 0.01 charges per monomer unit.

Fig. 3.a shows *in situ* PL spectra recorded from MEH-PPV at increasing potentials during the *p*-doping process. The black curve (bias potential η= 0.0 V) represents the PL emission of the polymer in the undoped state. The application of potentials beyond the doping onset results in a progressive quenching of the emission. The complete quenching is accomplished from a bias potential of 0.32 V (1.4×10^{19} charges cm^{-3}), a similar value observed for the polaron band saturation in UV spectra. The initial fluorescence can be

recovered after applying a potential below the oxidation onset, where the polymer recovers its semiconducting state.

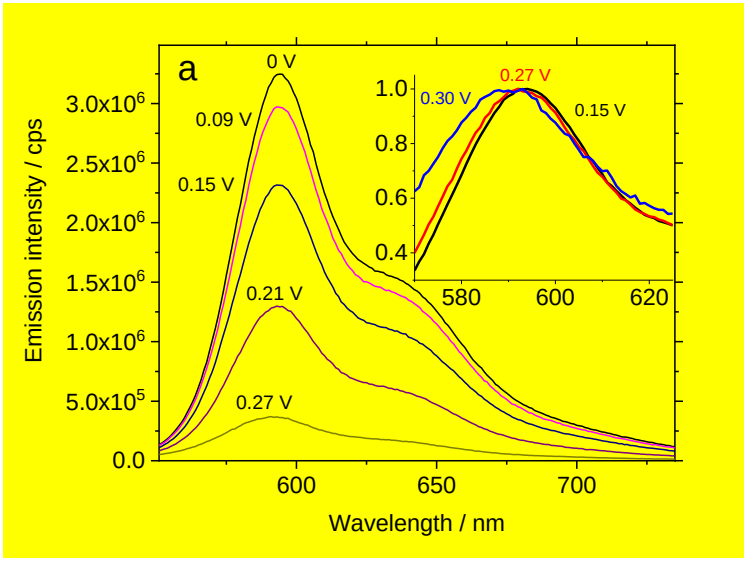

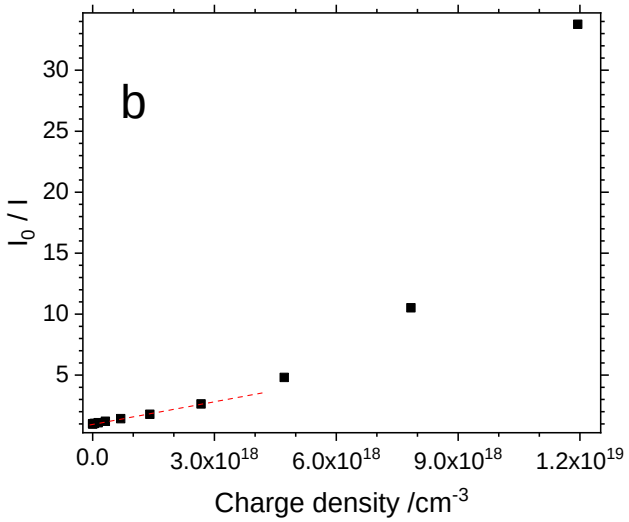

Figure 3. a) Evolution of the PL emission spectrum during the *p*-doping. Inset: Evolution of the normalized PL emission spectrum during the *p*-doping. The value of bias potential, η, is indicated close to the corresponding curve. (λ_{exc}= 500 nm). b) Electrochemical Stern-Volmer plot for the *p*-doping process of MEH-PPV.

The evolution of the shape of the PL spectrum can be appreciated in the inset to Fig. 3.a, where normalized emission spectra are presented at different doping potentials. The shape of fluorescent emission remains unaffected upon doping up to η= 0.15 V and the maximum stays at 594 nm, but it shifts to the blue when fluorescence is quenched at around a half of its initial value. This hypsochromic displacement reaches 8 nm at η= 0.32 V, a point where the emission from the polymer can be hardly detected. This behavior can be explained in terms of the fall down of exciton lifetime at high level of electrochemical doping. In the semiconducting state, the photogenerated excitons appear at different conjugated segments of the polymer and they are able to migrate toward low energy chromophores, i.e. red sites [28]. The generation of an increasing number of quenching centers promotes nonradiative paths for de-excitation and at high level of doping, the probability of a given exciton to reach a low energy site will be rather low. Under those conditions, the emission takes place exclusively from non-aggregated polymer chains which are blue sites.

The overall electrochemical quenching of PL can be modeled using approaches like those employed for solid-state fluorophores. When a photogenerated singlet exciton (S_1) finds a quencher (p) an annihilation process like that described in Eq. 2 can occur [29]:

$$S_1 + p \xrightarrow{k_q} S_0 + p + phonons \qquad (2)$$

being k_q the annihilation polaron-exciton rate constant. This bimolecular process competes with the monomolecular intrinsic de-excitation of excitons, described by a characteristic time constant equal to the lifetime of the photogenerated excited state, τ_0. Changes in the intensity

of emission in the presence of quenching sites generated by electrochemical doping can be modeled to obtain Eq. 3, an expression equivalent to the Stern-Volmer equation (the detailed derivation can be found in the supporting information in Section S2) [30]:

$$\frac{I_0}{I} = 1 + k_q \tau_0 [CD] \qquad (3)$$

being I and I_0 the fluorescent intensity in the presence and in the absence of the quencher, respectively, k_q the annihilation rate constant, τ_0 the characteristic lifetime for the photogenerated excited state and [CD] the quencher concentration (the injected charge density).

Fig. 3.b shows the electrochemical Stern-Volmer plot determined experimentally for MEH-PPV. At a low doping level, particularly below $CD = 3\times10^{18}$ cm^{-3}, the plot can be well fitted to a straight line, as expected for a time-independent quenching rate in a purely diffusion-controlled process (dynamic quenching). Such a linear trend reveals that a uniform distribution of emitters and quenchers is preserved over the PL lifetime, as a result of fast exciton diffusion [31]. Taking a fluorescence lifetime of $\tau_0 = 140$ ps for MEH-PPV [32], the quenching rate constant amounts to $k_q = 4.3\times10^{-9}$ cm^3 s^{-1}. This polaron-exciton quenching rate is nearly one order of magnitude lower than the exciton-exciton annihilation rate in this polymer [32]. It is worth mentioning that the difference between annihilation constants obtained from exciton-exciton and from electrochemical quenching of polyfluorene films lays in the same order of magnitude [31].

At a charge density higher than 3×10^{18} cm^{-3} the positive deviation observed in Fig. 3 is indicative of a combined quenching mechanism showing contributions of both diffusional collision and direct exciton-polaron quenching by resonant energy transfer [31]. If the

treatment is limited to the linear zone of the Stern-Volmer plot, k_q follows the Smoluchowski equation [33]:

$$k_q = 4\pi DR \qquad (4)$$

in which D is the mutual diffusion coefficient of donor and acceptor species ($D_{exciton}$ + $D_{polaron}$) and R is the exciton-polaron annihilation critical distance. Eq. 4 allows determining the exciton diffusion coefficient if the R parameter can be estimated. Gösele et al. [34] proposed Eq. 5 to calculate donor-acceptor critical distances under experimental conditions where the effect of exciton diffusion is significant:

$$R = 0.676\left(\frac{R_0^6}{\tau_0 D}\right)^{1/4} \qquad (5)$$

where R_0 is the transfer critical radius (or Förster critical radius) and the other symbols have been defined above. The Förster critical radius can be derived from experimental data using Eq. 6 [33,35]:

$$R_0(nm) = 0.0211[Q_D \kappa^2 n^{-4} J]^{\frac{1}{6}} \qquad (6)$$

here, Q_D is the emission quantum yield in the absence of energy transfer (Q_D= 0.08 [36]), κ^2 is the dipole orientation factor (0.476 for randomly oriented chromophores in solid state [30]), n is the average refractive index of the medium in the wavelength range where spectral overlap between donors and acceptors is significant, (n= 1.97 at 600 nm [37]). The spectral

overlap (J) can be evaluated from the emission and the absorbance spectra of doped MEH-PPV to obtain a Förster radius from Eq. 6 of R_0= 5.4 nm and the exciton-polaron critical distance is R= 4.7 nm, as derived from Eq. 5 (see section S3 in supporting information for details). The mutual diffusion coefficient can be obtained from the experimental value of k_q after the combination of Eqs. 4 and 5, resulting in D= 7.2×10^{-4} cm^2 s^{-1}. To determine the single diffusion coefficient of the exciton, $D_{exciton}$, it is essential to separate the contribution to D coming from its associated quasiparticle (polaron). Since the polaron mobility in PPV and related materials is typically within the range 10^{-11} to 10^{-5} cm^2 V^{-1} s^{-1} [38–40], at room temperature $D_{polaron}$ would be in the order of 10^{-13} to 10^{-7} cm^2 s^{-1}, as determined by the Einstein relation, considering that in doped conjugated polymers the electric field inside the material remains low thanks to charge compensation carried out by counterions [29]. Such a small figure makes the contribution to D of this quasiparticle negligible. A comparison between the obtained value and diffusion coefficients reported previously in the literature is shown in Table 1. It is worth mentioning that the average bibliographic value matches exactly the number derived from the analysis of the potential-dependent fluorescent emission carried out in the present work.

Table 1. Bibliographic data reported for exciton diffusion coefficient in MEH-PPV

Determination Method	$D_{exciton}$ /cm^2 s^{-1}	**Ref.**
Steady-state PL quenching by dyes	7.2×10^{-4}	[5]
Transient PL quenching by exciton-exciton annihilation	3×10^{-3}	[32]
Polymer/fullerene bilayer photocell	5.8×10^{-4}	[41]
Transient PL quenching by photooxidized sites	2.0×10^{-4}	[42]
Transient PL quenching polymer/fullerene bilayer	11×10^{-4}	[43]
Electrochemical PL quenching	7.2×10^{-4}	this work

4. Conclusions

In this work, we checked the applicability of combined *in situ* electrochemical UV-vis and fluorescence spectroscopies as tools for the characterization of absorption and photoluminescent emission properties of neutral and electrochemically-doped conjugated polymer emitters. This is performed by employing MEH-PPV as a model luminescent polymer system.

The *p*-doping process of the polymer can be accurately and reversibly controlled by electrochemical methods and results in an accumulation of positively charged holes of polaronic nature, which behave as quenching sites for photoluminescence. At low *p*-doping level, the quenching process fits a Stern-Volmer quenching model, controlled by the diffusive motion of photogenerated excitons along the conjugated backbone. From the slope of the Stern-Volmer plot and the exciton-polaron critical distance derived from exciton emission and polaron absorption spectral overlap, an exciton diffusion coefficient of 7.2×10^{-4} cm$^2\cdot$s^{-1} was estimated, in good agreement with the average value reported for MEH-PPV in the

literature. Electrochemical charge injection also brings about a progressive bleaching of the polymer ππ* transition and growth of the polaron absorption band, which is linear up to 0.01 charges per monomeric unit.

The successful analysis of the potential-dependent emission intensity of the fluorescence quenching allows this methodology to be proposed as an alternative, fast and powerful tool for the reliable measurement of exciton diffusion coefficients in conjugated polymer films, and therefore it encourages its future application to the study of a wider range of light-emitting systems.

5. Acknowledgements

This work was supported by Generalitat Valenciana (Conselleria de Educación, Investigación, Cultura y Deporte) project PROMETEO/2018/087 and Spanish Ministerio de Ciencia e Innovación (project PID2019-105923RB-I00).

6. References

1. Tamai, Y.; Ohkita, H.; Benten, H.; Ito, S. Exciton Diffusion in Conjugated Polymers: From Fundamental Understanding to Improvement in Photovoltaic Conversion Efficiency. *J. Phys. Chem. Lett.* **2015**, *6*, 3417–3428.

2. Tang, S.; Sandström, A.; Lundberg, P.; Lanz, T.; Larsen, C.; Van Reenen, S.; Kemerink, M.; Edman, L. Design rules for light-emitting electrochemical cells

delivering bright luminance at 27.5 percent external quantum efficiency. *Nat. Commun.* **2017**, *8*, 1190.

3. Menke, S.M.; Holmes, R.J. Exciton diffusion in organic photovoltaic cells. *Energy Environ. Sci.* 2014, *7*, 499–512.

4. Vacar, D.; Maniloff, E.S.; McBranch, D.W. Charge-transfer range for photoexcitations in conjugated polymer/fullerene bilayers and blends. *Phys. Rev. B - Condens. Matter Mater. Phys.* **1997**, *56*, 4573–4577.

5. Bjorgaard, J.A.; Köse, M.E. Amplified quenching of conjugated polymer nanoparticle photoluminescence for robust measurement of exciton diffusion length. *J. Appl. Phys.* **2013**, *113*, 203707.

6. Wang, X.; Groff, L.C.; McNeill, J.D. Multiple energy transfer dynamics in blended conjugated polymer nanoparticles. *J. Phys. Chem. C* **2014**, *118*, 25731–25739.

7. Furukawa, Y. Electronic absorption and vibrational spectroscopies of conjugated conducting polymers. *J. Phys. Chem.* **1996**, *100*, 15644–15653.

8. Montilla, F.; Ruseckas, A.; Samuel, I.D.W. Absorption cross-sections of hole polarons in glassy and beta-phase polyfluorene. *Chem. Phys. Lett.* **2013**, *585*, 133–137.

9. Scholes, D.T.; Yee, P.Y.; Lindemuth, J.R.; Kang, H.; Onorato, J.; Ghosh, R.; Luscombe, C.K.; Spano, F.C.; Tolbert, S.H.; Schwartz, B.J. The Effects of Crystallinity on Charge Transport and the Structure of Sequentially Processed F4TCNQ-Doped Conjugated Polymer Films. *Adv. Funct. Mater.* **2017**, *27*, 1702654.

10. Al-Kutubi, H.; Zafarani, H.R.; Rassaei, L.; Mathwig, K. Electrofluorochromic systems: Molecules and materials exhibiting redox-switchable fluorescence. *Eur. Polym. J.* 2016, *83*, 478–498.

11. Audebert, P.; Miomandre, F. Electrofluorochromism: from molecular systems to set-up and display. *Chem. Sci.* **2013**, *4*, 575–584.

12. Zhai, Y.; Zhu, Z.; Zhou, S.; Zhu, C.; Dong, S. Recent advances in spectroelectrochemistry. *Nanoscale* 2018, *10*, 3089–3111.

13. Kim, S.; You, Y. Highly Reversible Electrofluorochromism from Electrochemically Decoupled but Electronically Coupled Molecular Dyads. *Adv. Opt. Mater.* **2019**, 1900201.

14. Corrente, G.A.; Beneduci, A. Overview on the Recent Progress on Electrofluorochromic Materials and Devices: A Critical Synopsis. *Adv. Opt. Mater.* **2020**, *8*.

15. Čížková, M.; Cattiaux, L.; Mallet, J.M.; Labbé, E.; Buriez, O. Electrochemical switching fluorescence emission in rhodamine derivatives. *Electrochim. Acta* **2018**, *260*, 589–597.

16. Yen, H.J.; Liou, G.S. Design and preparation of triphenylamine-based polymeric materials towards emergent optoelectronic applications. *Prog. Polym. Sci.* 2019, *89*, 250–287.

17. Seo, S.; Shin, H.; Park, C.; Lim, H.; Kim, E. Electrofluorescence switching of fluorescent polymer film. *Macromol. Res.* 2013, *21*, 284–289.

18. Ding, G.; Zhou, H.; Xu, J.; Lu, X. Electrofluorochromic detection of cyanide anions using a benzothiadiazole-containing conjugated copolymer. *Chem. Commun.* **2014**, *50*, 655–657.

19. Beaujuge, P.M.; Fréchet, J.M.J. Molecular design and ordering effects in π-functional materials for transistor and solar cell applications. *J. Am. Chem. Soc.* **2011**, *133*, 20009–20029.

20. Schwartz, B.J. Conjugated polymers as molecular materials: how chain conformation and film morphology influence energy transfer and interchain interactions. *Annu. Rev. Phys. Chem.* **2003**, *54*, 141–72.

21. Montilla, F.; Pastor, I.; Mateo, C.R.; Morallon, E.; Mallavia, R.; Morallón, E.; Mallavia, R. Charge transport in luminescent polymers studied by in situ fluorescence spectroscopy. *J. Phys. Chem. B* **2006**, *110*, 5914–5919.

22. Santos, L.F.; Faria, R.C.; Gaffo, L.; Carvalho, L.M.; Faria, R.M.; Gonçalves, D. Optical, electrochemical and electrogravimetric behavior of poly(1-methoxy-4-(2-ethyl-hexyloxy)-p-phenylene vinylene) (MEH-PPV) films. *Electrochim. Acta* **2007**, *52*, 4299–4304.

23. Cardona, C.M.; Li, W.; Kaifer, A.E.; Stockdale, D.; Bazan, G.C. Electrochemical considerations for determining absolute frontier orbital energy levels of conjugated polymers for solar cell applications. *Adv. Mater.* **2011**, *23*, 2367–2371.

24. Holt, A.L.; Leger, J.M.; Carter, S.A. Electrochemical and optical characterization of p- and n-doped poly[2-methoxy-5-(2-ethylhexyloxy)-1,4-phenylenevinylene]. *J. Chem. Phys.* **2005**, *123*.

25. Fernandas, M.R.; Garcia, J.R.; Schultz, M.S.; Nart, F.C. Polaron and bipolaron transitions in doped poly(p-phenylene vinylene) films. *Thin Solid Films* **2005**, *474*, 279–284.

26. Candeias, L.P.; Grozema, F.C.; Padmanaban, G.; Ramakrishnan, S.; Siebbeles, L.D.A.; Warman, J.M. Positive charge carriers on isolated chains of MEH-PPV with broken conjugation: Optical absorption and mobility. *J. Phys. Chem. B* **2003**, *107*, 1554–1558.

27. Ho, P.K.H.; Thomas, D.S.; Friend, R.H.; Tessler, N. All-polymer optoelectronic devices. *Science (80-.).* **1999**, *285*, 233–236.

28. Martini, I.B.; Smith, A.D.; Schwartz, B.J. Exciton-exciton annihilation and the production of interchain species in conjugated polymer films: Comparing the ultrafast stimulated emission and photoluminescence dynamics of MEH-PPV. *Phys. Rev. B - Condens. Matter Mater. Phys.* **2004**, *69*, 035204.

29. van Reenen, S.; Vitorino, M. V; Meskers, S.C.J.; Janssen, R.A.J.; Kemerink, M. Photoluminescence quenching in films of conjugated polymers by electrochemical doping. *Phys. Rev. B* **2014**, *89*.

30. Valeur, B. *Molecular Fluorescence. Principles and Applications*; 1st ed.; Wiley-VCH Verlag GmbH, 2001; ISBN 3-527-29919-X.

31. Montilla, F.; Ruseckas, A.; Samuel, I.D.W. Exciton-Polaron Interactions in Polyfluorene Films with β-Phase. *J. Phys. Chem. C* **2018**, *122*.

32. Lewis, A.J.; Ruseckas, A.; Gaudin, O.P.M.; Webster, G.R.; Burn, P.L.; Samuel, I.D.W. Singlet exciton diffusion in MEH-PPV films studied by exciton-exciton

annihilation. *Org. Electron.* **2006**, *7*, 452–456.

33. Lakowicz, J.R. *Principles of Fluorescence Spectroscopy*; Plenum Press: New York, 2013; ISBN 0306412853.

34. Gosele, U.; Hauser, M.; Klein, U.K.A.; Frey, R. Diffusion and Long-Range Energy-Transfer. *Chem. Phys. Lett.* **1975**, *34*, 519–522.

35. Rolinski, O.J.; Birch, D.J.S. Determination of acceptor distribution from fluorescence resonance energy transfer: Theory and simulation. *J. Chem. Phys.* **2000**, *112*, 8923–8933.

36. Marchioni, F.; Chiechi, R.; Patil, S.; Wudl, F.; Chen, Y.; Shinar, J. Absolute photoluminescence quantum yield enhancement of poly(2-methoxy 5-[2′-ethylhexyloxy]-p-phenylenevinylene). *Appl. Phys. Lett.* **2006**, *89*, 061101.

37. Tammer, M.; Monkman, A.P. Measurement of the anisotropic refractive indices of spin cast thin poly(2-methoxy-5-(2′-ethyl-hexyloxy)-p-phenyl-enevinylene) (MEH-PPV) films. *Adv. Mater.* **2002**, *14*, 210–212.

38. Tuladhar, S.M.; Poplavskyy, D.; Choulis, S.A.; Durrant, J.R.; Bradley, D.D.C.; Nelson, J. Ambipolar Charge Transport in Films of Methanofullerene and Poly(phenylenevinylene)/Methanofullerene Blends. *Adv. Funct. Mater.* **2005**, *15*, 1171–1182.

39. Blom, P.W.M.; de Jong, M.J.M.; van Munster, M.G. Electric-field and temperature dependence of the hole mobility in poly(p-phenylene vinylene). *Phys. Rev. B* **1997**, *55*, R656–R659.

40. Jiang, X.; Harima, Y.; Zhu, L.; Kunugi, Y.; Yamashita, K.; Sakamoto, M.; Sato, M. Mobilities of charge carriers hopping between π-conjugated polymer chains. *J. Mater. Chem.* **2001**, *11*, 3043–3048.

41. Halls, J.J.M.; Pichler, K.; Friend, R.H.; Moratti, S.C.; Holmes, A.B. Exciton diffusion and dissociation in a poly(p-phenylenevinylene)/C60 heterojunction photovoltaic cell. *Appl. Phys. Lett.* **1996**, *68*, 3120–3122.

42. Yan, M.; Rothberg, L.J.; Papadimitrakopoulos, F.; Galvin, M.E.; Miller, T.M. Defect quenching of conjugated polymer luminescence. *Phys. Rev. Lett.* **1994**, *73*, 744–747.

43. Markov, D.E.; Tanase, C.; Blom, P.W.M.; Wildeman, J. Simultaneous enhancement of charge transport and exciton diffusion in poly(p-phenylene vinylene) derivatives. *Phys. Rev. B - Condens. Matter Mater. Phys.* **2005**, *72*, 045217.